RSC Advances

PAPER

View Article Online
View Journal | View Issue

Cite this: *RSC Adv.*, 2021, **11**, 918

Rapid and economic preparation of wearable thermotherapy pad based on simple cut-patterning of metal foil supported by plastic sheets†

Sung-Hun Ha[a] and Jong-Man Kim *[ab]

Stretchable and skin-mountable heaters have found application in the emerging industry of wearable thermotherapy devices. However, despite their excellent heating performances, most of them commonly suffer from complex, time-consuming, costly, or insufficiently reproducible fabrication processes. In this study, we report a simple, economic, and reproducible strategy to fabricate high-performance stretchable heaters based on facile cut-patterning of plastic sheet/metal foil/plastic sheet (PMP) structures. Further, this method can be executed without expensive materials or cumbersome material synthesis. The fabricated PMP heater is confirmed to exhibit excellent and uniform heating performance at a low voltage and satisfactory electrothermal stability even under high strain and repeated loads. Additionally, the proposed heater designs can be easily customized by simply changing the computer-aided design drawings during the cutting process, which also enables fabrication of devices with large area. The fabricated PMP heater is confirmed to be able to maintain conformal contact with target surfaces even under stretched conditions, inducing a fairly uniform temperature distribution. Finally, it is successfully demonstrated that a PMP heating band can be easily worn on the wrist and is capable of transferring enough heat to increase blood perfusion in the heated area even at a low voltage, highlighting its potential in wearable thermotherapy.

Received 1st July 2020
Accepted 15th December 2020

DOI: 10.1039/d0ra05728b

rsc.li/rsc-advances

Introduction

Thermotherapy is one of the most common and widely used techniques in physiotherapy, which plays an essential role in alleviating joint stiffness, reducing muscle spasms and inflammation, relieving pain, and increasing blood flow *via* the application of heat.[1–5] Mechanically flexible resistive heaters based on Joule heating have recently been considered as wearable components that can supply heat directly to target body parts for therapeutic purposes. In particular, such heaters are required to possess sufficient levels of mechanical stretchability coupled with electrical robustness to ensure intimate contact with curvilinear body contours and achieve low-loss transfer of constant heat to the wearers even under large-scale motion.

To date, diverse attempts have been carried out to develop highly stretchable and efficient heating devices for application in high-performance wearable thermotherapy devices.[6–27] Percolation networks comprising conductive materials (CMs) have been the most widely employed candidates as stretchable heating resistors primarily due to their inherent stretchability and relatively simple preparation.[6–14] The CMs that are usually utilized include carbon nanotubes (CNTs),[6] silver nanowires (AgNWs)[7–9] and nanofibers,[10] AgNW/CNT[11,12] and conductive polymer/reduced graphene oxide composites,[13] and super-aligned CNT sheets.[14] The conductive percolation networks can be easily integrated with elastomer and fabric substrates either by directly coating the CMs[6,7,10–13] or by transferring pristine or patterned CM networks onto stretchable substrates.[8,9,14] However, random morphologies of CM networks generally hinder the reproducibility and uniformity of the devices in terms of both fabrication and performance. Moreover, it has been reported that the electrothermal performance of these types of heaters degrade with increasing strain, predominantly due to the gradual loss of electrical pathways in their CM networks.[8,11,12]

Continuous metallic networks, prepared *via* the deposition of thin metal films on freestanding electrospun nanofiber networks followed by their transfer to elastomers, have been observed to simultaneously exhibit high electrical conductivity and excellent optical transmittance toward invisible wearable heaters.[15,16] However, even this approach was observed to suffer from issues related to random morphologies of the heating resistors. Further, device fabrication proved to be quite complex and expensive due to the presence of multiple processing steps

[a]*Department of Nano Fusion Technology and BK21 Plus Nano Convergence Technology Division, Pusan National University, Busan 46241, Republic of Korea*

[b]*Department of Nanoenergy Engineering and Research Center for Energy Convergence Technology, Pusan National University, Busan 46214, Republic of Korea. E-mail: jongkim@pusan.ac.kr*

† Electronic supplementary information (ESI) available. See DOI: 10.1039/d0ra05728b

including a high-vacuum process (*i.e.*, physical vapor deposition).

Conductive inks, synthesized with AgNWs[17] and liquid metal,[18] have been successfully patterned on elastomers *via* direct printing techniques to fabricate stretchable heaters with predetermined geometries of heating lines. However, this strategy is unsuitable for large-area fabrication and mass-production of devices due to the nature of the direct writing process.

In another approach, fibrous elastomers were coated using CMs (*e.g.*, CNT sheets[19] and copper NWs[20]) and then directly weaved in the form of a fabric to fabricate wearable textile heaters. Another type of the textile heaters was prepared *via* thermal carbonization of textile sheets and encapsulating them with elastomers.[21,22] However, the fabrication process is complex and time-consuming, and has hindered the practical application of such heaters.

In addition, considerable efforts have recently been devoted to developing wearable heaters based on stretchable architectures that do not depend only on the inherent stretchability of the constituent materials.[23–27] Such structural approaches are highly desirable in resistive heaters to stably maintain their electrothermal performances even under high strains, as they allow the dissipation of stress by preferentially inducing the deformation of the structure over that of the heating resistor up to a certain threshold of strain. Moreover, the structured heaters have been confirmed to be capable of maintaining intimate contact with body parts and evenly heating them, even during motion.

Other approaches have utilized conductive elastomeric composites by sculpting them into a mesh *via* a sequential molding process[23] or patterning them into a micro kirigami shape using a pulsed laser ablation technique.[24] These approaches require the strict control of the CN density to optimize the electrical, mechanical, and optical properties of devices. Further, ultrastretchable thermal patches, consisting of several rigid heating pads connected to each other using serpentine metal interconnections, have been prepared *via* a batch microfabrication process in a precise and reproducible manner.[25] However, the overall fabrication has proved to be quite complicated and expensive. Paper-based stretchable heaters have also been fabricated by shaping conductive papers into the serpentine[26] and kirigami layouts[27] *via* a facile paper-cutting process. Despite the straightforward cutting-based fabrication process, the cumbersome and time-consuming preparation of conductive papers remains a challenge for this technique.

In this study, we present a simple, rapid, cost-effective, reproducible, and scalable fabrication process of high-performance wearable heaters based on facile cut-patterning of plastic sheet/metal foil/plastic sheet (PMP) structures. In particular, aluminum (Al) foil was chosen to be the conductive material in the current work because, besides its inexpensive nature and ubiquity, it possesses excellent and uniform electrical properties and easy patterning *via* the simple cutting process. The fabricated PMP heater was observed to exhibit fast and low-voltage Joule heating (47.7 ± 0.9 °C at 3 V within 30 s) and uniform temperature distribution throughout the heating area at various input voltages. The creation of parallel cut patterns on the inherently rigid PMP structure allowed them to be stretched by up to >75% with no significant degradation in the electrothermal performance. Importantly, the stretchability of the device could be easily tuned by modulating the ratio of the dimension of the cutting parts to the total device length. The device was also verified to be electrically and mechanically robust enough to almost uniformly maintain the maximum temperature and a stable temperature distribution on the heated area even after repeated stretching cycles (10 000 cycles under 30% strain). In addition, it was confirmed that the device can be attached to targets while maintaining conformal contact with them, even when stretched, thereby resulting in low-loss heat transfer. Owing to its stable electrothermal and mechanical performance, it was concluded that the PMP heater could be successfully employed as a wearable thermotherapy pad to enhance blood perfusion.

Results and discussion

The proposed PMP heater consists of two layers: (1) a conductor layer consisting of serpentine-patterned Al foil/PET sheet and (2) a supporting PET sheet with parallel cut patterns. The device was fabricated *via* simple cut-patterning of the PMP structure, as schematically illustrated in Fig. 1(a). The heating parts and mechanical spring parts of the PMP heater were distinguished based on the parallel cut patterns created on the supporting PET sheets. Fig. 1(b) depicts the digital image of the fabricated PMP heater. The Al foil was patterned into a serpentine shape using a simple and programmable cutting process. Diverse geometries could also be potentially achieved in heater designs *via* this process by simply varying the CAD drawings. In addition, it is worth noting that Al foil is one of the most promising conducting materials for wearable heaters due to the following reasons: (1) it is extremely cheap (<0.5 $ per m^2 based on rough calculations) and (2) it exhibits excellent and uniform electrical properties ($R_s = 1.59 \pm 0.03$ mΩ sq^{-1}; Fig. S1 ESI†). The spring parts that had been deformed during the interconnection of the fixed heating parts upon stretching were also observed to have been defined well by simply aligning the parallel cut patterns with the serpentine-patterned heating resistor, as depicted in the magnified OM image in Fig. 1(c). It should be noted that 50 identical PMP heaters were observed to exhibit an average initial resistance (R_0) of ≈2.13 Ω with a very small standard deviation of only ≈0.05, as depicted in Fig. S2 (ESI†). In particular, the R_0 values of 47 out of the 50 devices were observed to lie within the narrow range of 2.05–2.2 Ω, highlighting the excellent fabrication reproducibility of the proposed heater. In addition to the simplicity and cost-effectiveness in material preparation and device fabrication, the noticeable reproducibility further facilitates the practical usage of PMP heaters in various applications, even as a disposable heating element.

Fig. 1(d) depicts the sequential digital images of the PMP heater in the initial, stretched, and released states. Upon application of strain, the device was stretched and the spring parts were deformed along the stretching direction. When the applied strain was removed, the heater structure completely recovered its initial shape owing to the considerable structural

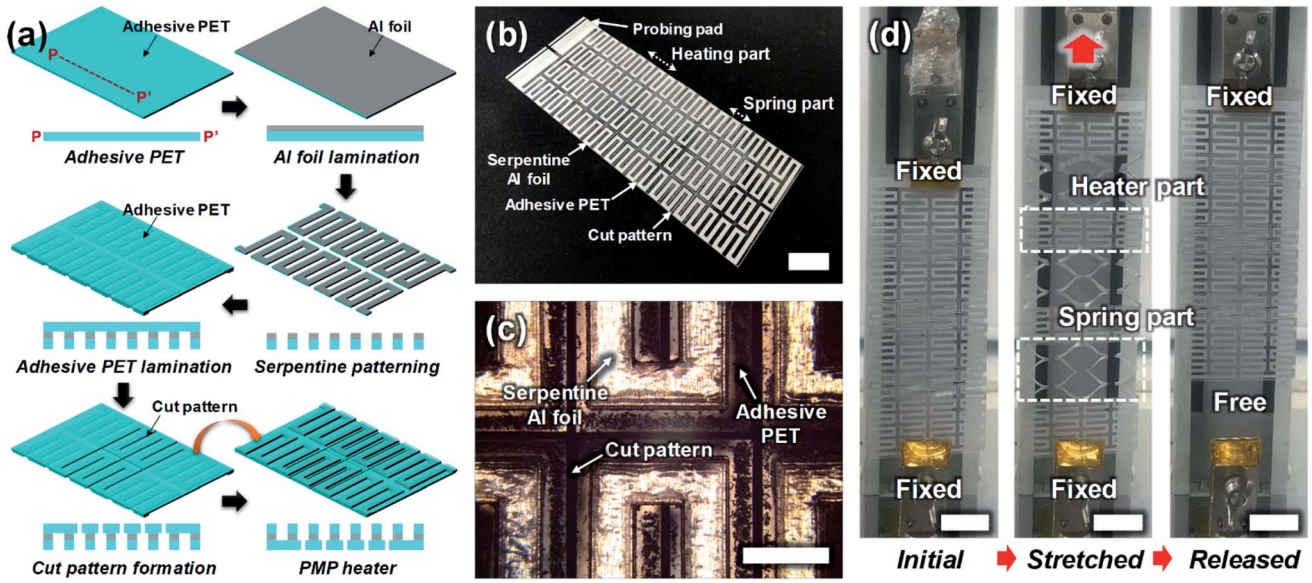

Fig. 1 Fabrication of stretchable heater based on cut-patterned plastic sheet/metal foil/plastic sheet (PMP) film. (a) Schematic illustration of the fabrication sequence, (b) digital image of the fabricated heater (scale bar: 20 mm), (c) magnified OM image of the cut pattern (scale bar: 2 mm), and (d) digital images of the device in the initial, stretched, and released states (scale bars: 20 mm).

reversibility of the constituent mechanical springs. This suggests that the PMP heater can accommodate itself along various curvilinear surfaces with different radii of curvature while maintaining conformal contact with them.

The stretchability of the PMP heater was controlled by simply varying the width of the cutting part (w_c). To investigate the effect of w_c on the electrical and mechanical properties of the fabricated heaters, three models of PMP heaters with different w_c (*i.e.*, $w_c = 6$, 12, and 18 mm) were investigated, as depicted in Fig. 2(a). Fig. 2(b) and (c) depict typical strain-dependent changes in force and normalized resistance (R/R_0), respectively, of the PMP heaters corresponding to varying w_c. The force–strain (F–S) curves of the devices displayed three strain ranges with distinct slopes (Fig. 2(b)). The initial slope corresponding to very small strains of <1% indicates that mechanical deformation was initiated in the springs of the device under the input strain (inset in Fig. 2(b)). When the strain was increased, the mechanical springs of the device deformed easily even under relatively small forces, thereby causing the F–S slope to decrease and remain gentle. Further increase in the input strain led to a steep increase in the F–S slope until one or more of the mechanical springs began to tear due to high stress concentrated at the junctions between the spring lines upon stretching. The three models of the heaters exhibited similar F–S curve patterns, but the maximum strain (ε_{max}) at which each device underwent mechanical failure was observed to increase with increase in w_c — the ε_{max} values were ≈40.1, 77.7, and 119.2% corresponding to w_c = 6, 12, and 18 mm, respectively. This phenomenon can be attributed to the fact that the maximum length of the device that can be stretched to before mechanical failure is proportional to the number of the parallel cut patterns.

As expected, the corresponding electrical properties of the heater models were retained without almost any change when stretched to ε_{max} (Fig. 2(c)). The R/R_0 values at ε_{max} were observed to be ≈0.986, 1.001, and 1.003 corresponding to w_c = 6, 12, and 18 mm, respectively. In particular, it is believed that the minimal differences between the initial and ε_{max} states are due to inevitable measurement errors, not due to deterioration of the electrical properties of heating resistors under strain. The excellent electrical robustness of the PMP structure might be attributed to the fact that the parallel cut patterns in the supporting PET sheets are deformed upon stretching while the serpentine-patterned Al foil is rarely structurally affected until the strain reaches ε_{max}.

More importantly, the electrical and mechanical behaviors of the device were also found to be highly reproducible, exhibiting insignificant deviations over at least five identical devices for each heater model ($\varepsilon_{max} \approx 40.1 \pm 0.6$, 77.7 ± 0.4, and 119.2 ± 0.5% and $R/R_0 \approx 0.993 \pm 0.006$, 1.003 ± 0.008, and 1.002 ± 0.001 corresponding to w_c = 6, 12, and 18 mm, respectively), as depicted in Fig. 2(d). In addition, the PMP heater (w_c = 12 mm) was also electrically and mechanically robust enough to maintain its initial resistance without significant degradation even when the device was subjected to 10 000 stretching cycles at 30% strain, as recorded in Fig. 2(e).

Considering the actual strain range that can be induced by human motions, the electrothermal performance of the PMP heater with w_c = 12 mm ($\varepsilon_{max} = 77.7 \pm 0.4$%) was evaluated and analyzed using a thermal imaging camera, as depicted in Fig. 3. Fig. 3(a) presents typical maximum temperature (T_{max}) profiles of the device in the initial state at various input voltages (V_{in}). Typically, the value of T_{max} value was observed to increase immediately when the voltage was applied to the device, almost reaching saturation within 30 s. The saturated T_{max} of the device was observed to reach 26.4–75.8 °C at low driving voltages of 1–5 V, verifying the proportional relationship between T_{max} and

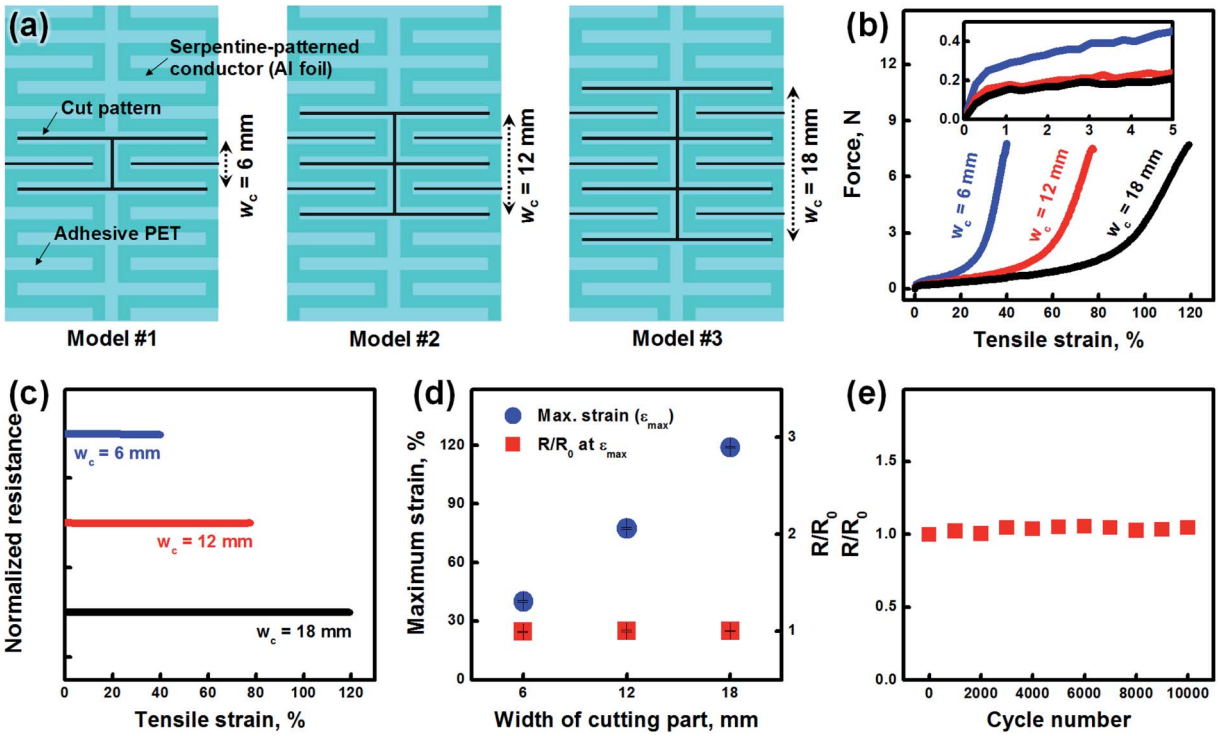

Fig. 2 Mechanical and electrical properties of the stretchable PMP heaters with different widths of the cutting part (w_c). (a) Schematic illustration of the heater design, (b) force–strain curve (inset: magnified waveforms in the initial region) and (c) normalized resistance (R/R_0) of the devices as a function of applied strain, (d) maximum strain (ε_{max}) before mechanical failure and R/R_0 value at ε_{max} for each heater model (w_c = 6, 12, and 18 mm), and (e) R/R_0 values of the device (w_c = 12 mm) in response to 10 000 stretching/releasing cycles under 30% strain.

V_{in}^2. It is worth noting that the electrothermal performance of the PMP heater can be further optimized by simply modulating the width and geometry of the heating resistor. In particular, in the context of wearable devices, power consumption of such heaters need to be fairly low during operation. The power densities required to raise the temperature of the PMP heater to 26.4–75.8 °C were observed to be as low as 0.82–20.4 mW cm^{-2} (heating area: 115 × 50 mm^2), thus representing its low power operation capabilities.

Moreover, the Joule heat was observed to be quite uniformly distributed throughout the heated area for each input voltage, as recorded in the thermal camera images presented in Fig. S3 (ESI†). To investigate the heat distribution on a heating part of the device (V_{in} = 3 V) more quantitatively, temperature profiles measured along the P–P' and Q–Q' axes were plotted in Fig. S4 (ESI†). Although the serpentine geometry of the heating resistor inevitably caused slight and periodic fluctuations of temperature, no significant temperature variation was detected on the heating part. Fig. 3(b) depicts the T_{max} values obtained from 15 identical heaters at various input voltages, which confirms the high reproducibility of the electrothermal performance of the proposed PMP heater. For example, the devices with an average T_{max} of ≈47.7 °C at 3 V exhibited a standard deviation as low as ≈0.9 °C.

To investigate the thermal characteristics of the PMP heater under strain, the dependence of T_{max} of the device (V_{in} = 3 V) on strain was recorded in real time in Fig. 3(c). The tested heater could be stretched by up to ≈76.4% while exhibiting a variation in T_{max} of less than 5.8% with respect to that at its initial temperature, representing a much higher resistance to mechanical deformations compared to heaters made of conductive nanomaterial percolation networks.[8] The slight decrease in T_{max} upon stretching can be attributed to the promotion of heat loss to ambient air caused by the gradual separation of the heating parts. Nevertheless, the temperature distribution on the heating parts still remained fairly uniform even when the device was stretched, as depicted in the sequential thermal camera images of the device in response to the applied strain in Fig. 3(d). This advantage can be attributed to the excellent electrical stability of the PMP structure under strain, as confirmed by the data presented in Fig. 2(c). Sequential digital images depicting the deformation process of the whole heater structure under strain have also been provided in Fig. S5 (ESI†). When the applied strain exceeded ε_{max}, T_{max} was observed to rapidly decrease with the gradual breaking of the mechanical springs. This process was also detected in different models of the PMP heaters in similar forms (Fig. S6 (ESI)†), suggesting that the device can be easily stretched by higher than 100% with no significant deterioration in the electrothermal performance by simply changing the cutting part design. Each heater model exhibited a somewhat different heat distribution over the entire device area upon stretching because the width of the heating part is changed depending on the change in w_c with respect to the fixed device size.

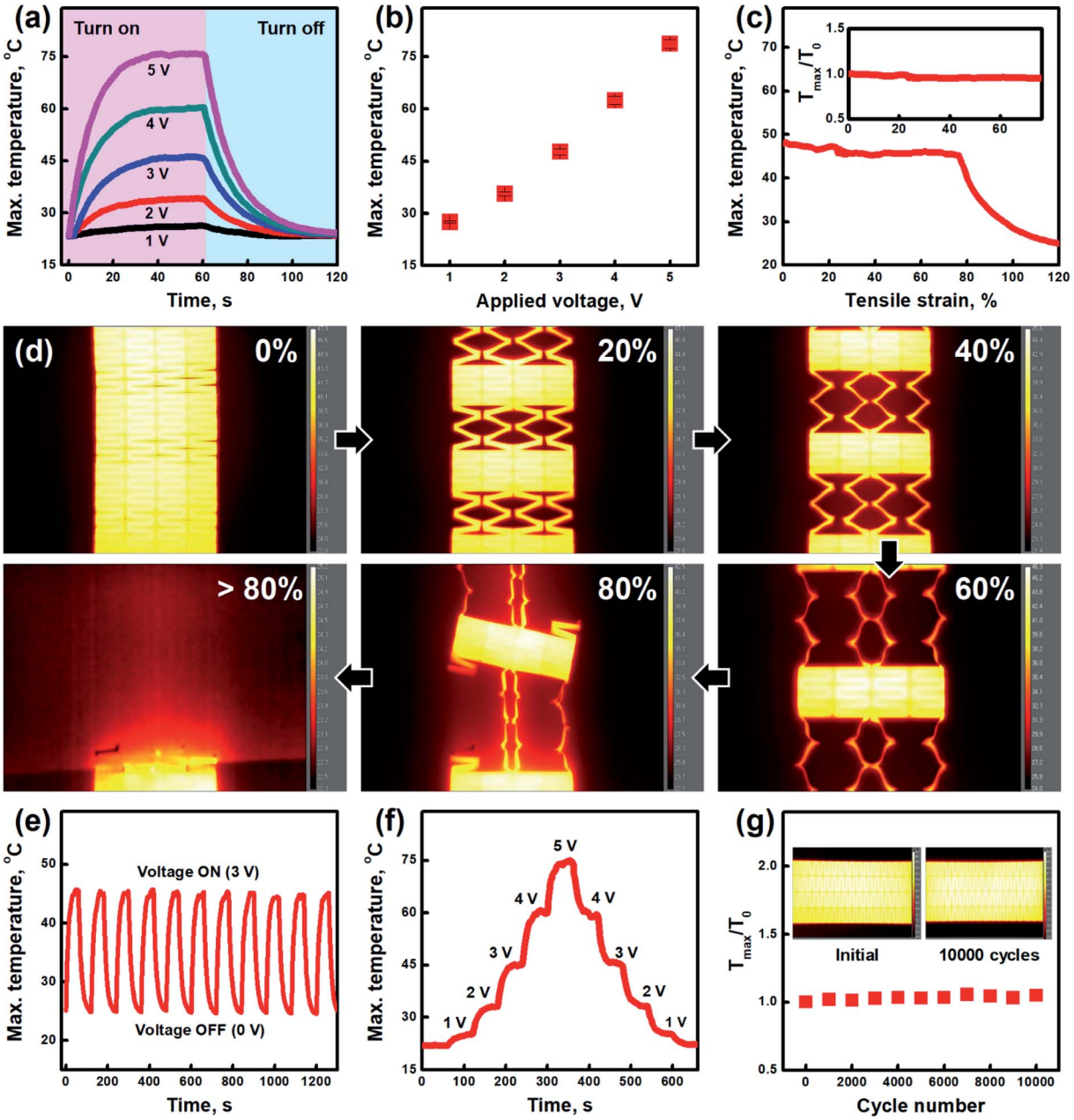

Fig. 3 Electrothermal performance of the stretchable PMP heater (w_c = 12 mm). (a) Time-dependent profile and (b) steady-state value of maximum temperature (T_{max}) of the heater as a function of applied input voltage (V_{in}), (c) strain-dependent variation in T_{max} (inset: normalized T_{max} (T_{max}/T_0) of the device before the mechanical failure) and (d) corresponding thermal camera images of the device at various strains (V_{in} = 3 V), time-dependent T_{max} profiles under the (e) repeated on/off operations (V_{in} = 3 V) and (f) stepped input voltages, and (g) T_{max}/T_0 of the device under 10 000 stretching/releasing cycles under 30% strain (V_{in} = 3 V) (inset: thermal camera images of the heater before and after the cyclic test).

Nevertheless, from an application point of view, it is important that the stretchability of the device can be easily modulated by simply changing w_c according to the application target. This also implies that the PMP heater can provide heat treatment over large areas of the body, even during motion.

Further, the PMP heater was observed to operate well even under dynamic conditions, as evidenced in Fig. 3(e) and (f). The device stably and reversibly responded to repeated on/off cycles with durations of 1 min (V_{in} = 3 V, Fig. 3(e)). The Joule heating performance of the device was also reliable enough to rapidly and precisely accommodate itself corresponding to sequential increases and decreases in the input voltage (1 V steps with durations of 1 min each) while indicating consistency in the results presented in Fig. 3(b) (Fig. 3(f)).

The Joule heating durability of wearable heaters is another essential prerequisite to their practical application. To investigate this characteristic for the proposed PMP heater, it was subjected to repeated stretching–releasing cycles. Fig. 3(g) depicts the normalized T_{max} (T_{max}/T_0, where T_0 is the temperature in the initial state) of the device during cyclic stretching

(10 000 cycles at 30% strain; V_{in} = 3 V). The measurement was performed once every 1000 cycles out of a total of 10 000 cycles. The electrothermal performance of the device was maintained at an almost constant level during the 10 000 stretching cycles. The uniform temperature distribution was also retained without considerable degradation during the 10 000 stretching cycles, compared to that in the initial state (inset in Fig. 3(g) and S7 (ESI)†). This desirable long-term heating stability can be attributed to the electrical and mechanical robustness of the proposed PMP structure against repetitive stretching, as confirmed by the data presented in Fig. 2(e). The experiment results suggest that the PMP heaters can be easily prepared in a fast, economic, scalable, and highly reproducible manner while exhibiting the mechanical and electrothermal performance comparable to wearable heaters based on stretchable architectures.[23–27]

In wearable thermotherapy, stretchable heaters need to be able to maintain close contact with curvilinear body parts as well as stably transfer heat to them even during various types of motion. In particular, unlike film-type heaters, stretchable structure-based devices inevitably tend to exhibit open spaces that cannot directly transfer Joule heat to the target surfaces as the structure is stretched. This might give rise to a nonuniform temperature distribution throughout the heating area. To address this issue, we attached the 20%-stretched PMP heater to a soft polymer substrate, which is used to mimic human skin, and investigated the transfer of heat at the open spaces in the springs (V_{in} = 3 V), as depicted in Fig. 4.

Fig. 4(a) and (b) depict the thermal camera images of the PMP heaters in the air and on the polymer, respectively. The Joule heat is observed to be much better distributed on the polymer around the edges of the heater structure, compared to that in the air, due to the conduction of heat from the heater to the polymer surface. To investigate this characteristic more quantitatively, we tracked temperature changes in the regions 'A' (heating part) and 'B' (open spring part) marked in Fig. 4(a) and (b), as depicted in Fig. 4(c) and (d), respectively. In the heating part (region 'A'), the temperature of the device on the polymer ($T_{polymer}$) tended to rise more slowly than that in the air (T_{air}) (Fig. 4(c)), potentially due to heat transfer to the polymer *via* conduction in the course of the heating process. In addition, $T_{polymer}$ was observed to be saturated at a higher value ($\approx$54.3 °C at 10 min) than T_{air} ($\approx$47 °C at 10 min). This can be attributed to the selective contact of a single side of the PMP heater with the polymer surface, resulting in lower overall heat flux from the heater to the ambient air. Meanwhile, in the open spring part (region 'B'), $T_{polymer}$ was observed to increase to $\approx$44.5 °C over 10 min, whereas T_{air} remained constant at $\approx$25.5 °C (Fig. 4(d)).

Fig. 4(e) depicts the temperature profiles scanned along the *P*–*P*′ lines marked in Fig. 4(a) and (b). The measurements were carried out 10 min after the application of 3 V to the devices. As expected, the PMP heater on the polymer exhibited a much smaller temperature variation between the heating and open spring parts ($\Delta T \approx$ 6.5 °C), compared to that in the air ($\Delta T \approx$ 22.8 °C). A similar trend was also observed for the 50%-stretched case, as shown in Fig. S8 (ESI†). However, it is thought that further quantitative investigation should be conducted to

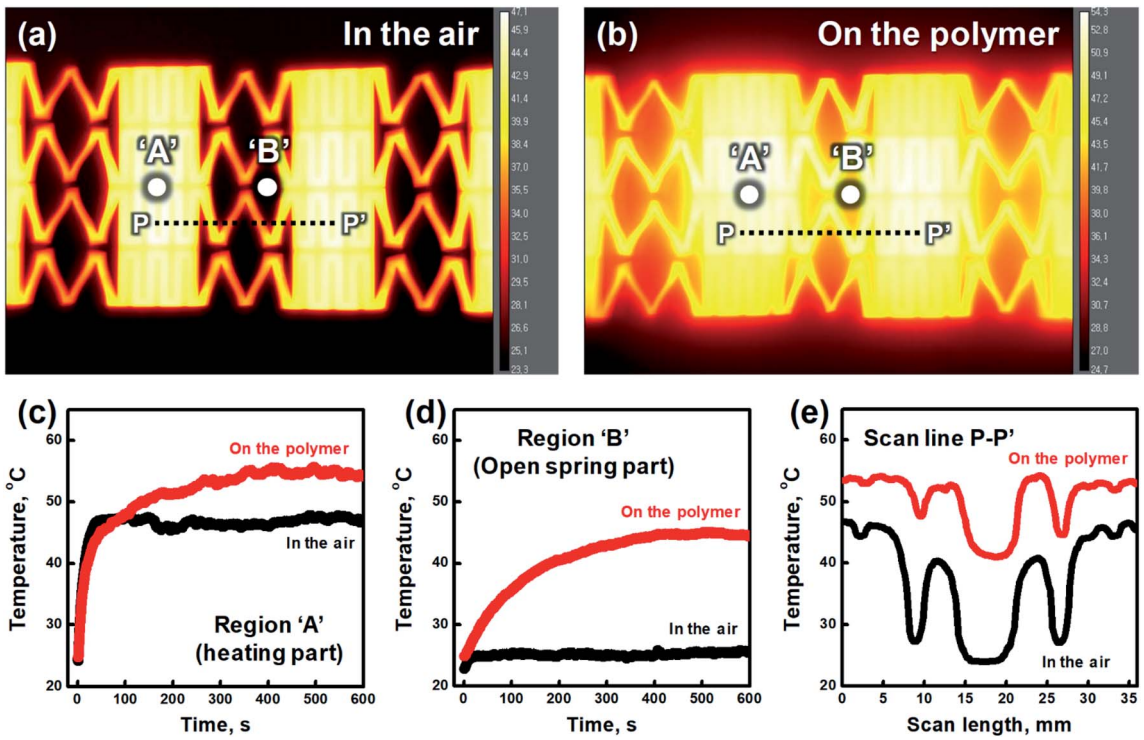

Fig. 4 Heat transfer behavior of the stretchable PMP heater (w_c = 12 mm). Thermal camera images of the 20%-stretched PMP heater (a) in the air and (b) on the polymer, time-dependent temperature profiles monitored at the regions (c) 'A' (heating part) and (d) 'B' (open spring part) marked in (a) and (b), and (e) temperature profiles scanned along the *P*–*P*′ lines marked in (a) and (b).

increase the practicality of the PMP heaters as a wearable thermotherapy device. The experimental results suggest that the stretchable PMP heater can stably and uniformly transfer heat to target surfaces even when the targets are deformed.

The excellent electrothermal performance in conjunction with high stretchability enables the proposed PMP heater to be easily affixed onto the wrist in the shape of a band and maintain conformal contact with it during upward and downward bending while simultaneously heating evenly, as depicted Fig. 5(a). In the initial state, the PMP heating band attached to the wrist exhibited a T_{max} of ≈40.7 °C at a driving voltage of 2.5 V that is directly applied to the device using a DC power supply. In this case, the Joule heating temperature of the device was observed to remain below 45 °C by limiting the input voltage to 2.5 V in order to protect the target skin from low-temperature burns.[17] It is also worth noting that the heating resistor is not in direct contact with the skin because it is sandwiched between two insulating sheets. T_{max} was maintained to be ≈40.7 and ≈41.2 °C during the upward and downward bending states, respectively. The temperature distribution of the PMP heater attached to other body parts (*e.g.*, elbow and knee joints) was also quite even without significant deviation over the entire heating area during the joint motions, as shown in Fig. S9 and S10 (ESI†). It should be noted that the fabrication strategy proposed in the present work can be easily extended to prepare a large-area PMP heater (230 × 130 mm^2; Fig. S11(a) (ESI)†).

The large-area heater required a higher driving voltage to raise its temperature to the target value (T_{max} ≈ 45 °C at an input voltage of ≈12.6 V; Fig. S11(b) (ESI)†), compared to the results presented in Fig. 3(b) and S2 (ESI).† This phenomenon can be attributed to the higher resistance (R_0 ≈ 10 Ω) of the longer heating resistor, which causes additional electrical energy to be required to maintain the target temperature because $Q \propto V_{in}^2/R$, where Q is the amount of heat. Nevertheless, the device was also observed to exhibit a uniform temperature distribution throughout the heating area, suggesting potential extensions to large-scale applications.

Finally, the practicality of the stretchable PMP heater in the context of therapeutic purposes was evaluated by applying the PMP heating band to the wrist of a volunteer and measuring the induced blood perfusion in that region. Fig. 5(b) presents the representative images obtained *via* laser Doppler imaging (LDI) analysis before and after heating the wrist (scan area: 15 × 15 mm^2) with the wearable PMP heater at 2.5 V. The LDI images indicate that the Joule heat transferred from the heater increased blood flow around the heated region by inducing vasodilation. In particular, the average blood perfusion increased by ≈131.6% after applying the heater, compared to that in normal conditions, as depicted in Fig. 5(c), thereby enabling possible alleviation in pain and stiffness at the joint.

Thus, the experimental observations confirmed that the proposed PMP heater is highly feasible as an efficient, low-cost and low-voltage heat source that can stably provide uniform Joule heat throughout the target body parts even during motion for practical wearable thermotherapy.

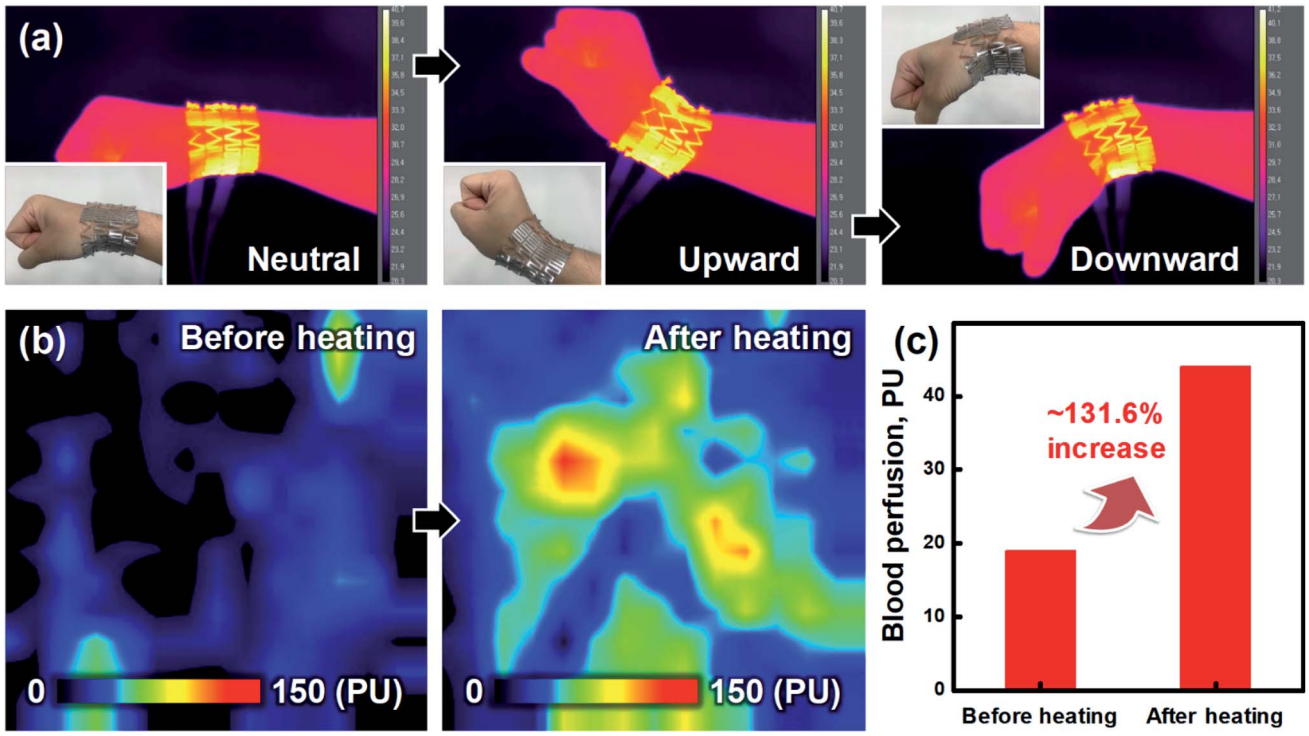

Fig. 5 Wearable thermotherapy application. (a) Thermal camera images of the PMP heater attached to the wrist in the initial, upward, and downward bending states (V_{in} = 2.5 V) (inset: corresponding digital images), and (b) Doppler color images indicating blood perfusion at the wrist and (c) average blood perfusion before and after heating with the PMP heater (V_{in} = 2.5 V; scan area: 15 × 15 mm^2).

Conclusions

In conclusion, we have fabricated a high-performance stretchable heater based on cut-patterned PMP structures *via* a simple, rapid, low-cost, reproducible, and potentially scalable method and successfully demonstrated its potential as a wearable thermotherapy pad. The electrothermal response characteristics of the fabricated PMP heater were observed to be fast, uniform, and efficient enough to evenly raise the temperature of the target region to up to 47.7 ± 0.9 °C at 3 V within 30 s. The PMP heater could be stretched to higher than 100% without any significant loss in the electrothermal performance *via* design optimization of the cutting (mechanical spring) parts (average $\varepsilon_{max} \approx 40.1$, 77.7, and 119.2% corresponding to $w_c = 6$, 12, and 18 mm, respectively) and was observed to transfer heat fairly evenly to the target surface even when stretched ($\Delta T \approx 6.5$ °C between the heating and spring parts under 20% strain). In addition, the Joule heating performance of the PMP heater was also verified to be highly robust even under dynamic conditions (cyclic on/off operation and sequential excitation) and repeated stretching cycles (10 000 cycles at 30% strain). The PMP heating band worn on the wrist was demonstrated to induce a significant increase in blood perfusion by ≈131.6% *via* sufficient heating around the wrist at a low voltage of 2.5 V. The observations confirm that the PMP heaters can be used as an efficient heating source in wearable thermotherapy applications owing to their excellent and reliable heating performance in conjunction with their mechanical stretchability and stability.

Experimental

Materials and device fabrication

20 μm-thick Al foils (Lotte Aluminium) and ≈125 μm-thick laminating polyethylene terephthalate (PET) sheets (Royal Sovereign) were purchased from a local supermarket and stationery store, respectively.

To fabricate the PMP heaters, an A4-sized PET sheet was first laminated onto an Al foil using a film laminator (EXCELAM II-355Q, GMP) under a temperature of 90 °C and then patterned into a serpentine shape using a computer-controlled cutting plotter (Cameo, Silhouette) based on a computer-aided design (CAD) schematic. Another PET sheet was laminated onto the serpentine-patterned structure such that the Al foil resistor was sandwiched between the PET sheets. The device fabrication was completed by creating parallel cut patterns on the second PET sheet.

Characterization

The structure of the fabricated heater was investigated using an optical microscope (OM; BX60M, Olympus). A computer-interfaced motorized stage (JSV-H100, JISC) was used to apply tensile strain to the device while recording the corresponding force and electrical resistance (R) using a push–pull force gauge (HF-10, JISC) and digital multimeter (34465A, Keysight Technologies), respectively. The electrothermal properties of the PMP heaters were evaluated and analyzed using a thermal imaging camera (T630sc, FLIR). A direct current power supply (K1205, Vupower) was used to apply the input voltage to the device. A four-point probe (CMT-SR2000N, Advanced Instrument Technology) was used to measure the sheet resistance (R_s) of the Al foil laminated with a PET sheet.

Blood perfusion at the wrist of a volunteer, in the initial and heated states, was measured (15 × 15 mm^2) using a laser Doppler imaging (LDI) system (PeriScan PIM3, Perimed AB). The LDI system basically evaluates the Doppler shift related to the velocity of the blood cells, which occurs when a transmitted laser beam reacts with moving blood cells. The measurement in the heated state was performed by heating the wrist for 10 min and scanning it using a wearable PMP heating band at an applied voltage of 2.5 V.

Conflicts of interest

There are no conflicts to declare.

Acknowledgements

This work was supported by a 2-Year Research Grant of Pusan National University.

Notes and references

1 M. Dehghan and F. Farahbod, *J. Clin. Diagn. Res.*, 2014, **8**, LC01.
2 S. Michlovitz, L. Hun, G. N. Erasala, D. A. Hengehold and K. W. Weingand, *Arch. Phys. Med. Rehabil.*, 2004, **85**, 1409.
3 S. F. Nadler, K. Weingand and R. J. Kruse, The Physiologic Basis and Clinical Applications of Cryotherapy and Thermotherapy for the Pain Practitioner, *Pain Physician*, 2004, **7**, 395.
4 S. Ochiai, A. Watanabe, H. Oda and H. Ikeda, *J. Phys. Ther. Sci.*, 2014, **26**, 281.
5 L. Brosseau, K. A. Yonge, V. Welch, S. Marchand, M. Judd, G. A. Wells and P. Tugwell, *Cochrane Database Syst. Rev.*, 2003, CD004522.
6 J. Yan and Y. G. Jeong, *Mater. Des.*, 2015, **86**, 72.
7 J.-G. Lee, J.-H. Lee, S. An, D.-Y. Kim, T.-G. Kim, S. S. Al-Deyab, A. L. Yarin and S. S. Yoon, *J. Mater. Chem. A*, 2017, **5**, 6677.
8 S. Hong, H. Lee, J. Lee, J. Kwon, S. Han, Y. D. Suh, H. Cho, J. Shin, J. Yeo and S. H. Ko, *Adv. Mater.*, 2015, **27**, 4744.
9 S. Yao, J. Yang, F. R. Poblete, X. Hu and Y. Zhu, *ACS Appl. Mater. Interfaces*, 2019, **11**, 31028.
10 J. Jang, B. G. Hyun, S. Ji, E. Cho, B. W. An, W. H. Cheong and J.-U. Park, *NPG Asia Mater.*, 2017, **9**, e432.
11 J. Ahn, J. Gu, B. Hwang, H. Kang, S. Hwang, S. Jeon, J. Jeong and I. Park, *Nanotechnology*, 2019, **30**, 455707.
12 H. Kim, M. Seo, J.-W. Kim, D.-K. Kwon, S.-E. Choi, J. W. Kim and J.-M. Myoung, *Adv. Funct. Mater.*, 2019, **29**, 1901061.
13 R. Zhou, P. Li, Z. Fan, D. Du and J. Ouyang, *J. Mater. Chem. C*, 2017, **5**, 1544.
14 Y. Lee, V. T. Le, J.-G. Kim, H. Kang, E. S. Kim, S.-E. Ahn and D. Suh, *Adv. Funct. Mater.*, 2018, **28**, 1706007.

15 B. W. An, E.-J. Gwak, K. Kim, Y.-C. Kim, J. Jang, J.-Y. Kim and J.-U. Park, *Nano Lett.*, 2016, **16**, 471.
16 P. Li, J. Ma, H. Xu, X. Xue and Y. Liu, *J. Mater. Chem. C*, 2016, **4**, 3581.
17 Z. Cui, Y. Han, Q. Huang, J. Dong and Y. Zhu, *Nanoscale*, 2018, **10**, 6806.
18 Y. Wang, Z. Yu, G. Mao, Y. Liu, G. Liu, J. Shang, S. Qu, Q. Chen and R.-W. Li, *Adv. Mater. Technol.*, 2019, **4**, 1800435.
19 Y. Li, Z. Zhang, X. Li, J. Zhang, H. Lou, X. Shi, X. Cheng and H. A. Peng, *J. Mater. Chem. C*, 2017, **5**, 41.
20 Y. Cheng, H. Zhang, R. Wang, X. Wang, H. Zhai, T. Wang, Q. Jin and J. Sun, *ACS Appl. Mater. Interfaces*, 2016, **8**, 32925.
21 M. Zhang, C. Wang, X. Liang, Z. Yin, K. Xia, H. Wang, M. Jian and Y. Zhang, *Adv. Electron. Mater.*, 2017, **3**, 1700193.
22 C. Wang, M. Zhang, K. Xia, X. Gong, H. Wang, Z. Yin, B. Guan and Y. Zhang, *ACS Appl. Mater. Interfaces*, 2017, **9**, 13331.
23 S. Choi, J. Park, W. Hyun, J. Kim, J. Kim, Y. B. Lee, C. Song, H. J. Hwang, J. H. Kim, T. Hyeon and D.-H. Kim, *ACS Nano*, 2015, **9**, 6626.
24 P. Won, J. J. Park, T. Lee, I. Ha, S. Han, M. Choi, J. Lee, S. Hong, K.-J. Cho and S. H. Ko, *Nano Lett.*, 2019, **19**, 6087.
25 A. M. Hussain, E. B. Lizardo, G. A. T. Sevilla, J. M. Nassar and M. M. Hussain, *Adv. Healthcare Mater.*, 2015, **4**, 665.
26 B. Sadri, D. Goswami, M. S. de Medeiros, A. Pal, B. Castro, S. Kuang and R. V. Martinez, *ACS Appl. Mater. Interfaces*, 2018, **10**, 31061.
27 N.-S. Jang, K.-H. Kim, S.-H. Ha, S.-H. Jung, H. M. Lee and J.-M. Kim, *ACS Appl. Mater. Interfaces*, 2017, **9**, 19612.